

Ketogenic diet slows down mitochondrial myopathy progression in mice

Sofia Ahola-Erkkilä¹, Christopher J. Carroll¹, Katja Peltola-Mjösund¹, Valtteri Tulkki¹,
Ismo Mattila², Tuulikki Seppänen-Laakso², Matej Orešič², Henna Tynismaa¹
and Anu Suomalainen^{1,3,*}

¹Research Program of Molecular Neurology, Biomedicum-Helsinki, University of Helsinki, Helsinki 00290, Finland,
²VTT Technical Research Centre of Finland, Espoo FI-02044 VTT, Finland and ³Department of Neurology, Helsinki,
University Central Hospital, Helsinki, Finland

Received November 12, 2009; Revised and Accepted February 16, 2010

Mitochondrial dysfunction is a major cause of neurodegenerative and neuromuscular diseases of adult age and of multisystem disorders of childhood. However, no effective treatment exists for these progressive disorders. Cell culture studies suggested that ketogenic diet (KD), with low glucose and high fat content, could select against cells or mitochondria with mutant mitochondrial DNA (mtDNA), but proper patient trials are still lacking. We studied here the transgenic Deletor mouse, a disease model for progressive late-onset mitochondrial myopathy, accumulating mtDNA deletions during aging and manifesting subtle progressive respiratory chain (RC) deficiency. We found that these mice have widespread lipidomic and metabolite changes, including abnormal plasma phospholipid and free amino acid levels and ketone body production. We treated these mice with pre-symptomatic long-term and post-symptomatic shorter term KD. The effects of the diet for disease progression were followed by morphological, metabolomic and lipidomic tools. We show here that the diet decreased the amount of cytochrome *c* oxidase negative muscle fibers, a key feature in mitochondrial RC deficiencies, and prevented completely the formation of the mitochondrial ultrastructural abnormalities in the muscle. Furthermore, most of the metabolic and lipidomic changes were cured by the diet to wild-type levels. The diet did not, however, significantly affect the mtDNA quality or quantity, but rather induced mitochondrial biogenesis and restored liver lipid levels. Our results show that mitochondrial myopathy induces widespread metabolic changes, and that KD can slow down progression of the disease in mice. These results suggest that KD may be useful for mitochondrial late-onset myopathies.

INTRODUCTION

Mitochondrial diseases are a clinically and genetically heterogeneous group of disorders, with manifestations varying from late-onset myopathies and neurodegeneration to fatal infantile multisystem diseases. These diseases can be caused by mutations either in mitochondrial DNA (mtDNA) or in nuclear genes encoding mitochondrial proteins. mtDNA encodes 13 polypeptides, which are all catalytically crucial subunits of the respiratory chain (RC) complexes, as well as the tRNAs and rRNAs required for mitochondrial translation. Any defect of mtDNA, therefore, affects the activity of RC and impairs oxidative phosphorylation (OXPHOS) and ATP

production. As mtDNA is dependent on nuclear genes for its maintenance, mtDNA defects can be caused by a primary mtDNA mutation or a nuclear mutation causing secondary depletion or mutagenesis of mtDNA. The morphological sign of RC deficiency is the finding of cytochrome *c* oxidase (COX)-negative muscle fibers in histological analysis of a skeletal muscle sample, and morphologic abnormalities of mitochondrial ultrastructure, including crista deformations, inclusions and swelling.

Presently, no therapy is available for mitochondrial RC deficiencies (1). Therapy trials have been hampered by the difficulty to collect large enough study groups of a single disease entity, because of the heterogeneity of the human disease

*To whom correspondence should be addressed at: Biomedicum-Helsinki, r.C523B, Haartmaninkatu 8, 00290 Helsinki, Finland. Tel: +358 947171965; Fax: +358 919125610; Email: anu.wartiovaara@helsinki.fi

phenotypes and genotypes. Even when a disease is caused by a defined mtDNA mutation, the proportions of mutant and wild-type (WT) mtDNAs vary in different patients, leading to a wide spectrum of different manifestations. Good disease models are therefore an essential tool for testing treatment strategies.

We have previously created a mouse model for late-onset mitochondrial myopathy (2), which overexpress ubiquitously a dominant patient mutation of Twinkle, the nuclear-encoded replicative helicase of mtDNA (duplication of amino acids 353–365) (2,3). In humans, the homologous mutation causes autosomal dominant progressive external ophthalmoplegia (4), with generalized muscle weakness and COX-negative muscle fibers, as well as accumulation of large-scale mtDNA deletions. The mice manifest at 1 year of age typical histological and genetic features of mitochondrial myopathy, including COX-negative fibers showing swollen, enlarged and morphologically abnormal mitochondria in electron microscopy, and accumulation of mtDNA deletions (hence the name ‘Deletor’), mimicking closely the human disease. The disease progresses slowly without considerably affecting the lifespan of the mice. Therefore, the model is well suited for testing of therapy options for the disorder.

Ketogenic diet (KD) has been proposed as a possible treatment for mitochondrial disorders (5–7). This diet consists of a low glucose and high lipid content, stimulating lipid utilization by mitochondrial beta-oxidation and ketone body production in the liver. Ketone bodies are high-energy-content compounds that can be utilized as an energy source by the brain, heart and skeletal muscle. Increased supply of ketone bodies increases transcript levels of genes associated with OXPHOS, TCA cycle and glycolysis, and has been shown to increase mitochondrial biogenesis and the number of mitochondria in hippocampal neurons (8). In cell culture, ketone body treatment shifted heteroplasmy in favor of WT mtDNA molecules (5), and the authors suggested KD as a possible therapy for patients with heteroplasmic mtDNA disorders. Recently, KD was reported to reduce the frequency of epileptic seizures in child patients with epilepsy and RC complex deficiency, and in Alpers syndrome, however, the diet was unable to stop the disease progression in all 15 reported patients (6,7). In these human studies, the patient materials were too small and heterogeneous to allow firm conclusions of the effects of KD on RC deficiency. The effects of KD on mutant mtDNA *in vivo* have not been studied. These issues prompted us to test high-fat, carbohydrate-restricted KD in Deletor mice with a homogeneous genetic background and with late-onset mitochondrial myopathy.

RESULTS

We have previously shown that the Deletor mice develop COX-negative and succinate dehydrogenase (SDH)-positive muscle fibers, as a result of their mitochondrial RC dysfunction, at the age of 10–12 months (2). A gender difference of the original Deletor phenotype was detected: Deletor males had three times more COX-negative fibers in their *quadriceps femoris* muscle (QF) than the females at 14 months of age (5.6 ± 0.9 versus $1.9 \pm 0.2\%$, respectively; $P < 0.0001$), and about 2.5 times more mtDNA deletions ($P = 0.002$), suggesting a later

initiation or slower disease progression in females. Therefore, in the treatment trial, we concentrated on the more severely affected male Deletors. To test whether KD can affect the disease onset and severity, we gave WT and Deletor mice a pre-symptomatic, long-term KD, as well as a control diet (CD) with similar food appearance, from the age of 4 months until the age of 14 months, after which the mice were sacrificed and the diet consequences studied. We also tested whether KD has an effect upon disease manifestation and pursued a second trial starting at the manifestation of the disease (12 months). These mice were also sacrificed at the age of 14 months.

KD decreases the amount of COX-negative muscle fibers in male Deletor mice

We counted approximately 2000 fibers per each mouse muscle section cut from a standardized site of the QF (Supplementary Material, Fig. S1). The long-term pre-symptomatic KD showed a clear effect: the Deletor male mice on CD had 1.5 times more COX-negative fibers than the Deletors on KD (5.6 ± 0.3 versus $3.8 \pm 0.4\%$, respectively; $P = 0.0077$) (Fig. 1A). No COX-negative fibers were found in WT mice at the age of 14 months.

KD did not affect mtDNA deletion load or mtDNA copy number in Deletor mice, but induced mitochondrial biogenesis

Multiple mtDNA deletions are a key finding in the Deletor mouse muscle (2) and are thought to underlie the RC dysfunction and COX-negative muscle fibers. Because KD decreased the number of COX-negative fibers, we studied the amount of mtDNA deletions by a semi-quantitative PCR method. KD did not significantly affect the amount of mtDNA deletions (Fig. 1B). At the age of 14 months, the WT mouse muscle showed no mtDNA deletions. Previously, KD has been shown to increase mitochondrial biogenesis and mtDNA copy number (8,9). Accordingly, we detected about 1.5-fold increase of mtDNA copy number in WT mouse muscle after KD ($P = 0.02$). However, the Deletors showed no change in mtDNA amount after KD (Fig. 1C). Improved COX status could be due to overall up-regulation of RC complexes or increased complex activity. However, KD did not have a major effect on complex I levels (data not shown) or its activity in the skeletal muscle of the Deletor or the WT male mice (Supplementary Material, Fig. S2). KD induced mitochondrial biogenesis in the Deletor mice, and showed a trend for induction also in the WT mice on KD when measured as citrate synthase activity, a mitochondrial matrix enzyme (Fig. 1D).

KD rescued the muscle mitochondrial ultrastructure in Deletor mice

We performed electron microscopic studies on the skeletal muscle of Deletor and WT male mice and found that mitochondrial ultrastructure was clearly affected by KD diet (Fig. 2). We have previously shown that Deletor muscle shows morphologically abnormal large mitochondria, with distorted cristae and electron-dense inclusions (2) (Fig. 2F)

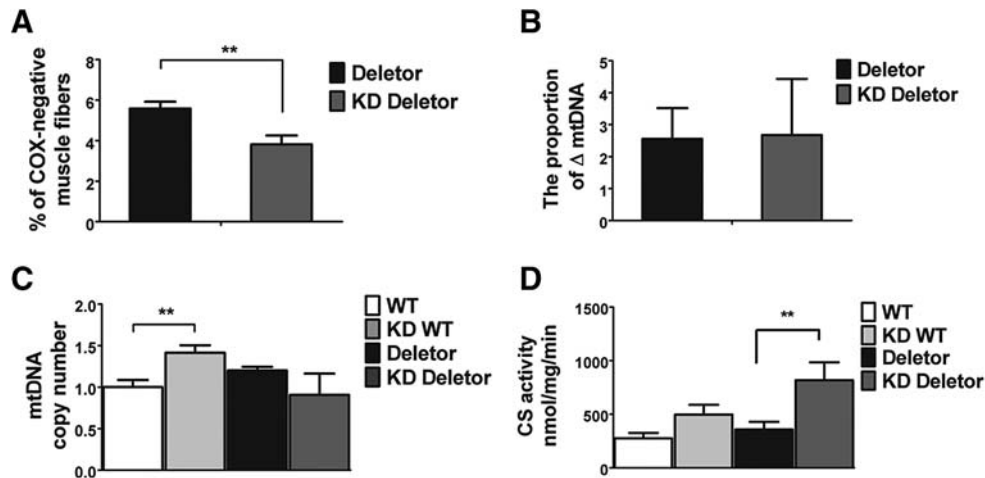


Figure 1. Effects of KD on muscle phenotype, mtDNA and citrate synthase activity in late-onset myopathy mice. KD-fed mice showed decreased amounts of COX-negative muscle fibers in QF, compared with the untreated group (A). mtDNA deletion load did not change after the KD (B). mtDNA copy number increased in WT mouse muscle after KD, but was unaffected in Deletors (C). Results in (C) are expressed as fold change compared with WT CD mice which were designated as 1. (D) Citrate synthase (CS) activities measured from the QF. KD-fed Deletor mice showed induced citrate synthase activity, and the KD-fed WT mice showed a similar trend. $**P < 0.01$.

similar to patients with the same mutation (4), as well as induced mitophagy, with readily identifiable autophagosomes. Remarkably, mitochondrial ultrastructure was normal in the KD-fed Deletors (Fig. 2H). The proportion of mitochondria with an electron-dense matrix, an indicator of actively metabolizing mitochondria, was clearly increased in both Deletors and WT mice on KD (Fig. 2C, D, G and H), as well as the mitochondrial volume and number considerably increased. The mitochondria were redistributed within the muscle fiber, being accumulated subsarcolemmally close to blood vessels, in both WT and Deletors (Fig. 2C, D, G and H), and the volume and matrix density of intermyofibrillar mitochondria were increased. Intramuscular fat droplets were often found to be surrounded by mitochondria (Fig. 2H). No autophagosomes were detected in the KD-fed Deletors.

Metabolomic and lipidomic consequences of KD

We performed metabolomic and lipidomic analysis of the Deletor male mouse plasma and lipidomic analysis of the muscle, with and without KD, to have a global view of the metabolic consequences of the disease and the diet. Ketone bodies are produced in liver mitochondria from acetyl-CoA, which is generated by beta-oxidation of fatty acids. Acetyl-CoA is converted to acetic acid (ACA), and further to 3-hydroxybutyric acids (3-HBAs) and low amounts of acetone. KD resulted in a trend for plasma ACA increase in WT mice ($P = 0.055$), but 3-HBA was not altered (Fig. 3A). The Deletor mice on normal diet had decreased levels of 3-HBAs in their plasma compared with their WT littermates ($P = 0.02$), suggesting increased peripheral ketone body utilization or reduced synthesis in the liver (Fig. 3A). KD-fed Deletors, however, had WT levels of these ketone bodies. KD increased plasma cholesterol levels in both Deletors and WT ($P < 0.05$) mice (Fig. 3A). Of the various lipid classes analyzed, Deletor mice showed decreased phosphatidylcholine levels ($P < 0.01$) in their plasma, but increased levels in their muscle ($P < 0.05$) compared with WT mice levels (Fig. 3B).

After KD, however, both the muscle and plasma levels of phosphatidylcholine were similar to WT. Sphingomyelin levels were increased in Deletor muscle compared with WT levels ($P < 0.0001$), and KD induced further increase in both WT and Deletor, reaching similar levels (Fig. 3B). Plasma triacylglycerol levels were increased in Deletors after KD ($P < 0.05$) (Fig. 3B). These results show that KD feeding normalized widespread changes in lipid status and ketone-body levels in late-onset myopathy mice.

Plasma amino acid levels were systematically elevated in Deletor mouse plasma compared with WT mice (Fig. 3C), but only glycine ($P = 0.005$) and serine ($P = 0.04$) were significantly increased. Remarkably, KD-fed mice showed WT levels of all other amino acids except leucine, glutamine and ornithine, showing that the KD also improved disease-associated deranged amino acid levels.

Deletor mice are resistant to diet-induced obesity

KD increased the weight of all mice, but the Deletors were partially resistant to the high-fat-diet-associated weight gain (Fig. 4A). The Deletor mice on KD weighed significantly less than WT mice on KD already after 1 week of the diet ($P < 0.05$, and after 40 weeks of the diet $P = 0.002$). We confirmed that the Deletors and the WT mice consumed similar amounts of food and their fecal fat content was similar (data not shown), indicating normal food intake and absorption. KD increased the amount of fecal lipids of both the Deletors and WT mice, and, overall, mice on KD ate less (by weight of chow) than mice on CD. As the high-fat, low-sucrose diet causes obesity (10), we monitored the physical performance of the mice during the diet with Rotarod and treadmill tests. KD did not affect the performance of the mice, except in very obese WT males on KD ($P < 0.05$) (Supplementary Material, Fig. S3). Long-term KD did not induce the expression levels of uncoupling protein 3, the isoform of the skeletal muscle, linked to protection of lipid-induced oxidative stress in the muscle (Supplementary Material, Fig. S4).

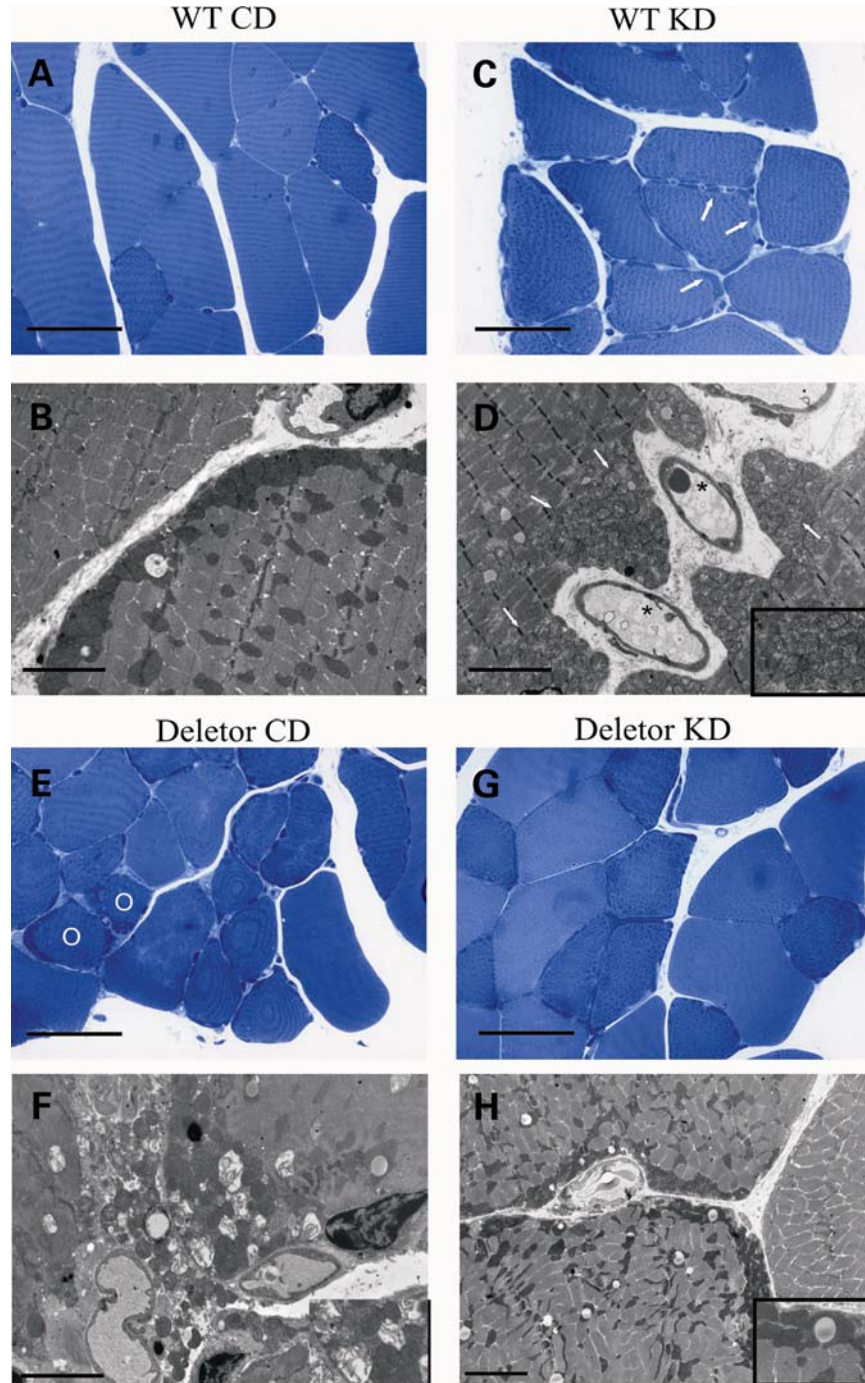


Figure 2. Effect of KD on WT and Deletor muscle morphology. (A–D) KD increased mitochondrial biogenesis (arrow) in the skeletal muscle of WT male mice especially around the blood vessels (asterisk). Deletor CD mice showed ragged red fiber-like muscle fibers (circle) (E) and mitochondria with distorted structure and cristae (F), which were not seen in Deletor KD mice (G and H). Fat droplets were found to be surrounded by mitochondria (H) (bottom right-hand box). Scale bar in (A), (C), (E) and (G) 50 μ m and in (B), (D), (F) and (H), 5 μ m.

The liver phenotype of the Deletors is rescued by KD

Deletor mice had less intracellular fat in the liver than their WT littermates on CD (Fig. 4B). However, after KD-feeding, Deletor liver fat levels were similar to WT mice on CD. For the WT mouse liver, high-fat-containing KD was highly damaging: the mice had large lipid pools in their liver

(Fig. 4B), associated with inflammation and fibrosis, with increases in plasma aspartate aminotransferase, alanine aminotransferase and lactate dehydrogenase levels (Supplementary Material, Table S1). These results suggest that the Deletor tissues benefit from introduction of high-energy sources, ketone bodies and fat, whereas in tissues with normal mitochondrial function, an overload of these is severely damaging.

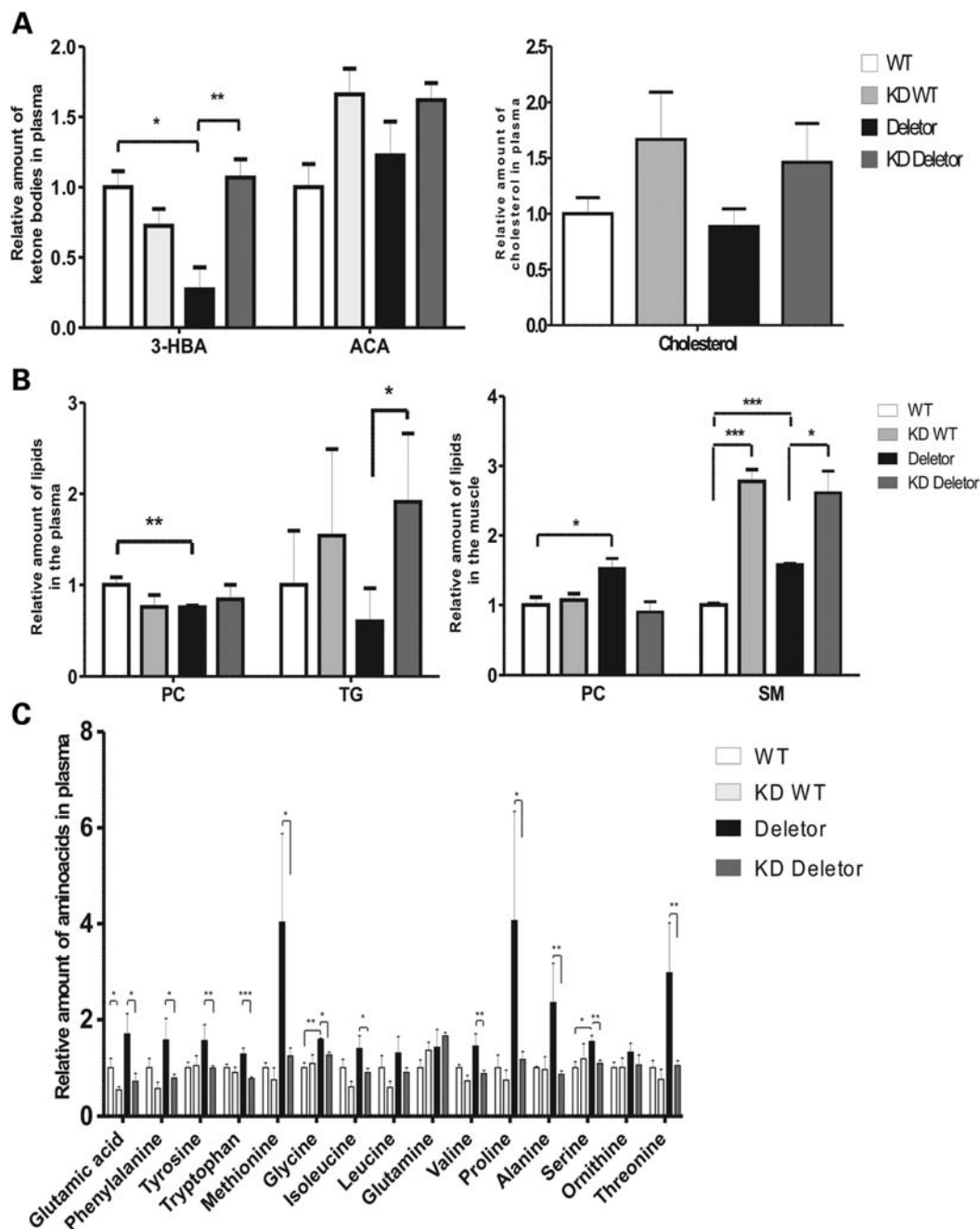


Figure 3. Effects of KD on metabolic changes in Deletors. (A) Deletor male mice showed decreased levels of 3-HBAs in their plasma compared with their WT littermates. KD rescued this phenotype. KD increased plasma ACA and cholesterol levels. (B) Deletor mice had decreased levels of phosphatidyl choline (PC) in their plasma and increased levels of PC and sphingomyelin (SM) in their muscle. KD also rescued these phenotypes but increased plasma triacylglycerol (TG) levels in Deletor and WT mice. (C) Deletor mice plasma amino acids were elevated, but only serine and glycine were elevated significantly. KD decreased the levels of most of the amino acids to the level of WT mice. * $P < 0.05$, ** $P < 0.01$, *** $P < 0.001$.

Effect of post-symptomatic KD mimics long-term KD for Deletor mice

Long-term KD ameliorated the disease phenotype of Deletors when started early in the pre-symptomatic phase. We then studied whether the diet affects the phenotype as a treatment to the disease when started after disease manifestation. Deletor and WT female and male mice were fed with CD

until the age of 12 months, and then switched to KD at the age of 12 months for 2 months, and sacrificed at 14 months. KD male Deletors were resistant to weight gain already after 2 weeks of the diet (Fig. 5A), and after 9-week diet, at the age of 14 months, their weight was 84% of that of WT mice ($P < 0.01$). There was no difference in female mouse weights during the study. Food consumption was similar in Deletors and in WT mice in both genders (data not shown).

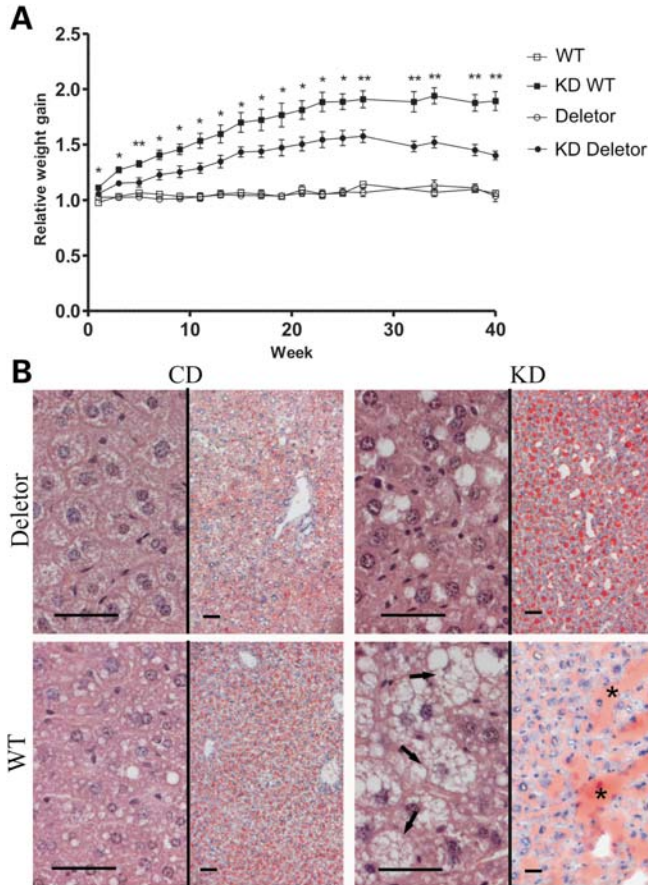


Figure 4. Effects of KD on weight and hepatic lipids. (A) The weight gain of the mice on KD or CD; weight proportional to the starting weight. Deletor mice are partially resistant to diet-induced obesity. (B) The liver of the Deletor mice lacked intracellular lipid droplets (lipids white in hematoxylin–eosin staining, upper left panel in CD), and showed reduced lipids in Oil Red O staining (lipids red; upper right panel in CD), compared with controls (lower left panels). On KD, Deletors showed WT-like lipids (upper right panels), whereas WTs on KD showed large lipid pools (asterisk) and extensive intracellular fat droplets (arrow). Scale 50 μ m. * P < 0.05 and ** P < 0.01.

The post-symptomatic KD treatment resulted in a decreasing trend of the number of COX-negative fibers in the Deletor males (mean 4.4% in KD and 6.2% in CD; P = 0.07), and a significant decrease in females (0.9% in KD and 1.9% in CD; P = 0.001) (Fig. 5B). We also tested the mtDNA deletion load in skeletal muscle, but it was unaffected by this post-symptomatic KD (data not shown), similar to the findings in the long-term, pre-symptomatic KD. mtDNA amounts in both study groups with KD showed an increasing trend, but this did not reach significance (Fig. 5C).

DISCUSSION

Mitochondrial disorders are the most common group of inherited metabolic disorders in humans, but effective therapies to slow down disease progression are not available. KD has been suggested to potentially reduce epileptic attacks in mitochondrial encephalopathies (6,7), but the human patient study groups have been small and heterogeneous. We studied the

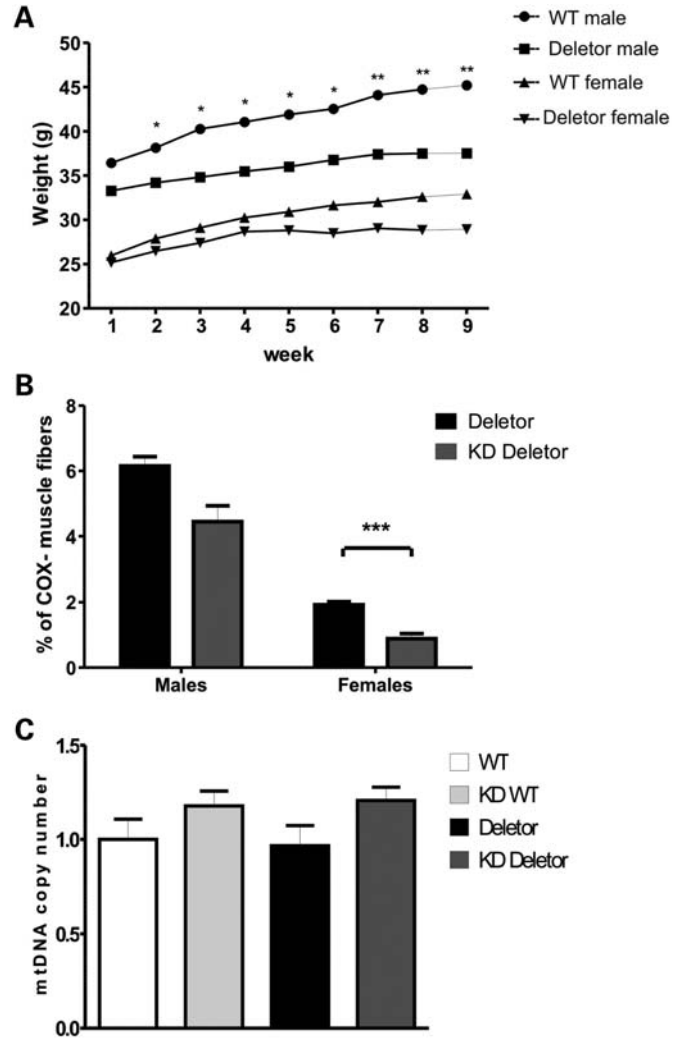


Figure 5. Effects of post-symptomatic (2 months) KD for WT and Deletor mice. (A) On a post-symptomatic KD, Deletor male mice showed reduction in weight gain already after 2 weeks of diet. (B) Quantification of COX-negative muscle fibers. Male Deletor mice showed a decreasing trend of COX-negative fibers, and the female Deletor mice had less COX-negative muscle fibers after post-symptomatic KD. * P < 0.05, ** P < 0.01 and *** P < 0.001. (C) Quantification of mtDNA copy number after post-symptomatic KD. mtDNA was unaffected by the diet in both Deletors and WT male mice.

effects of KD on a mouse model with late-onset progressive mitochondrial myopathy. Our results show that KD can induce mitochondrial biogenesis, slow down the disease progression and reduce the amount of COX-negative muscle fibers when given pre-symptotically. The diet may have a similar effect even if started at the time of the first symptoms as our post-symptomatic study showed. Furthermore, the KD improved the levels of a wide variety of different metabolic parameters, including different lipid classes, amino acids and ketone bodies. When testing physical performance and a wide range of physiological metabolic parameters, we did not find any indications for KD to be harmful for the Deletor mice with late-onset mitochondrial myopathy, whereas for WT mice it caused obesity and severe liver steatosis.

Previously, in cultured cells carrying single mtDNA deletions, ketone bodies added to the growth medium reduced

the proportion of mutant mtDNA molecules, suggesting that KD could counter-select for cells with high mutant mtDNA amount (5). In the Deletor mice, COX-negative fibers are associated with the accumulation of multiple mtDNA deletions owing to a dominant nuclear mutation in the gene encoding the Twinkle helicase. However, in KD-fed Deletors, in spite of the low amount of COX-negative fibers, the mutant mtDNA level was not significantly reduced nor was the mtDNA copy number significantly increased when analyzed in total muscle sample. Therefore, KD did not induce a significant selection for WT mtDNA in post-mitotic skeletal muscle.

We show here that KD has a remarkable effect on mitochondrial ultrastructure in skeletal muscle. Importantly, the KD-fed Deletors lacked all the mitochondrial abnormalities typical for mitochondrial myopathies in humans and mice, i.e. swelling, crista deformities and inclusions. KD activated oxidative metabolism in the skeletal muscle of both Deletors and WT mice, with increased number and volume of mitochondria with dense active matrices, which was accompanied by increased mtDNA amount only in WT mice but not in Deletor mice. The mitochondria in KD-fed Deletors were normal looking, in spite of the fact that the mice had partial COX deficiency and mtDNA deletions. This suggests that even subtle primary mitochondrial dysfunction can affect the energy metabolic mode of the skeletal muscle, probably shifting it to favor glycolysis in normal carbohydrate-rich diet. However, lipids can be utilized only through beta-oxidation in the mitochondria, and if they are the major fuel available, cells are forced to use mitochondria for ATP production by beta-oxidation. This strongly suggests that the type of nutrition can modulate the metabolic mode and physiological consequences of mitochondrial dysfunction and disease progression. Further, the metabolic shift can partially compensate for primary mitochondrial dysfunction.

Recently, PGC1- α induction and administration of PPAR-panagonist bezafibrate were shown to induce mitochondrial biogenesis and improve the RC phenotype of mice with severe COX deficiency (11). As KD in the present study also led to increased mitochondrial biogenesis, the mechanism could have been related to PGC1 induction. However, at 14 months, neither PGC1- α nor β was increased at the transcript level (data not shown). This suggests that either the induction of PGC1 was an early event, which was not seen after 10 months of KD or KD activated oxidative metabolism by another mechanism.

Skeletal muscle protein is a major energy source in limited nutritional state. In the Deletor muscle, mitophagy was induced (2), muscle proteins degraded and the mice had increased amounts of free amino acids in their serum, which suggested either increased proteolysis or decreased amino acid degradation (manuscript in preparation). KD-fed Deletors did not show induced mitophagy when studied by electron microscopy, and had similar serum-free amino acid levels as the WT mice, indicating inhibition of protein catabolism.

KD was harmful to WT mice, resulting in large pools of lipid and steatosis-associated inflammation in the liver. Increased amount of lipid vesicles in the liver was also found in a study where mice were fed with KD for 5 weeks (12). However, KD-fed Deletor livers mimicked closely those of the WT mice on a normal diet, i.e. showed no fat

pools, indicating utilization of the dietary fats. The lack of liver fat in the untreated Deletors had many potential consequences, including a decrease in ketone body synthesis. Logically, KD restored ketone body levels in the Deletors to the WT level, along with the hepatic lipid levels. Furthermore, liver is the site of synthesis for plasma lipids and lipoproteins. A major phospholipid, phosphatidylcholine, as well as triacylglycerols were low in Deletor plasma and the muscle showed also abnormal phospholipid levels. These results show that the lack of lipids in Deletor liver may have a profound effect on global lipid homeostasis. Importantly, KD restored these defects to the WT level in Deletors.

Kang *et al.* (6) gave KD to 14 child patients with single or combined RC deficiencies manifesting as epileptic encephalopathies, with no defined genetic diagnosis. The authors reported that epileptic seizures were especially reduced in the patients with Complex I deficiencies, sometimes allowing the patients to withdraw from other epilepsy medication. However, KD did not prevent fatal progression of the disease (6,7). Effect on CI deficiency can be expected, as beta-oxidation increases electron flow through CII, by-passing partly CI. Our Deletors, with multiple mtDNA deletions, show partial CI deficiency (2). Our study shows that induction of mitochondrial biogenesis by KD, boosting the function of defective RC, may be beneficial in cases with mild RC deficiency. However, the effects of inducing mitochondrial biogenesis in severe deficiencies, such as early-onset encephalomyopathies, remain to be studied in relevant animal models.

In conclusion, we show here that a high-fat diet has multiple positive effects on late-onset mitochondrial myopathy in mice, and slows down the disease progression. At the cellular level, KD down-regulated disease-associated protein catabolism, restored hepatic lipid levels and thereby ketone body synthesis and normalized lipid homeostasis. Interestingly, the diet, which was highly damaging for WT mice, was well tolerated by the Deletor mice, which showed no diet-associated adverse effects. These findings strongly suggest that the type of energy source can considerably modify the energy metabolism of skeletal muscle in RC defects, and that induction of oxidative metabolism may partially compensate RC deficiency. Studies testing low-carbohydrate, high-fat diet in late-onset mitochondrial myopathy patients are thus warranted.

MATERIALS AND METHODS

This work was approved by the Helsinki University animal care committee, and all experiments were done in accordance with good practice of handling laboratory animals. Twinkle^{dupl} transgenic mice, i.e. Deletor mice (2), and their WT littermates were used in this study. These mice carry as transgene, the mouse *Twinkle*-cDNA under a human β -actin promoter inserted into the genome. The cDNA carries a duplication mutation, an in-frame duplication of amino acids 353–365, corresponding to a dominant human patient mutation (4). The Deletor mice from the FVB/N background were backcrossed with C57BL/6. Female and male mice from generation F7, all offspring of one transgenic Deletor male, were chosen for the long-term study. In backcrossings, generation F10 is considered a pure strain. The long-term study comprised 20 WT mice

(10 males) and 19 Deletor mice (10 males), heterozygous for the duplication mutation. Eleven WT (six males) and 13 Deletor mice (eight males) from generations 10–11 were chosen for the short-term study. Animals were housed one or two per cage in a temperature-controlled (21°C) room with a 12 h light/dark cycle and ~60% relative humidity.

In the long-term study, Deletor and WT mice of 3–4 months of age were introduced an *ad libitum* KD (D05052004, Research Diets, Inc., New Brunswick, NJ, USA) or an *ad libitum* CD (Research Diets, Inc.). In the short-term post-symptomatic study, all the mice were introduced an *ad libitum* KD at the age of 12 months. KD consisted of fat 89.5 kcal%, carbohydrate 0.1 kcal% and protein 10.4 kcal% and CD of fat 11.5 kcal%, carbohydrate 78.1 kcal% and protein 10.4 kcal%. Both diets contained equal calories from soybean oil and the KD also contained primex fat, which is hydrogenated cottonseed oil and soybean oil and provides a high concentration of *trans* fatty acids. Mice had free access to water and chow (*ad libitum*). At the age of 14 months, the mice from both studies were anesthetized, blood was collected by cardiac puncture and the mice were sacrificed by cervical dislocation. Mice were fasted for 24 h before sacrifice to ensure the blood sample comparability. During the course of the study, two mice (one Deletor on KD, one WT on KD) were terminated for poor condition.

The body weight of the mice was determined regularly every second or third week and at the same time their general condition was observed by individual examination. To determine the chow consumption and intestinal fat absorption, daily chow consumption and fecal fat content were measured in both studies. In the long-term study, the chow eaten by 11 ketogenic and nine control mice was weighted daily for four consecutive days 1 week before the mice were sacrificed. The feces were collected during a 3-day period simultaneously with the chow-consumption study from eight KD- and seven CD-eating mice. During the post-symptomatic study, chow was weighted once every week during the whole study from all the animals and daily chow consumption was evaluated based on the week's average. Feces were homogenized with scissors and dried in +70°C for 1 h. Approximately, 0.1 g of dried sample was diluted into 2 ml 2:1 chloroform:methanol and heated in a sealed tube at +70°C for 30 min to dissolve lipids. The chloroform-methanol solution was separated in a weighed tube and evaporated overnight in a fume hood. The remaining residual material was weighed, proportioned to the fecal weight and assigned as total lipid (modified from Folch *et al.* (13)).

Mice in the long-term study were tested with Rotarod and treadmill at the beginning of the diet, twice during the diet period and 1 week before the end of the experiment to monitor well-being and physical exercise capacity. In the Rotarod test, the mice walked on a rotating rod (Ugo Basile, Biological Research Apparatus) with a starting speed of 6 rpm, followed by constantly accelerating rotation speed. The time of falling from the rod was recorded and the best of three consecutive attempts was chosen for further analysis. The treadmill test (Exer-6M Treadmill, Columbus Instrument) was performed with a starting speed of 7 m/min for 2 min, which then accelerated by 2 m/min after every 2 min. If the mice stopped running, they were encouraged to run by

gently pushing with a hand or with a light electrical stimulus. Mice ran until exhaustion. Only running scores over 2 min were chosen for further analysis to ensure that mice began to run.

Morphologic analysis

Samples were collected from the liver and QF. QF and a piece of liver were embedded with O.C.T Compound Embedding Medium (Tissue-Tek®) and frozen in isopentane/liquid nitrogen. Frozen tissue sections (12 µm) from QF were stained with simultaneous COX and SDH staining. Frozen tissue sections of 8 µm from QF and liver were stained with Oil Red O. The slides were fixed in formic calcium (1:10:1 concentrated formalin:aqua:10% calcium chloride) and then incubated in Oil Red O solution for 10 min. Oil Red O stock solution (1 mg/ml in isopropanol) was made by heating the reagent and alcohol at 56°C for 30 min. Fresh working solution was made from cooled stock solution and aqua (3:2). Solution was mixed well, let to stand for 5 min, filtrated and used within few hours. The nuclei were stained with Mayer's hematoxylin for 3 min. Stained sections were analyzed by light microscopy (Axioplan 2 Universal Microscope, Zeiss). COX-SDH stained muscles were inspected and abnormal muscle fibers were scored. From QF muscle, the three most severely affected fields were chosen from the ×50 magnification, photographed and the COX-negative, COX-negative and SDH-positive and normal fibers were counted. From each sample, approximately 2000 cells were counted in total. The proportion of COX-negative and normal fibers was calculated. For plastic embedding, muscle samples were fixed in 2.5% glutaraldehyde for 1.5 h, treated with 1% osmium tetroxide, dehydrated in ethanol and embedded in epoxy resin. Semithin (1 µm) sections were stained with methyl blue (0.5% w/v) and boric acid (1% w/v). For transmission electron microscopy, ultrathin (60–90 nm) sections were cut on grids and stained with uranyl acetate and lead citrate.

mtDNA deletion analysis

To determine the mtDNA deletion loads, long-range mtDNA PCR was performed. Primers were located near the 16S and ND1 gene region, which lies in a region that is usually retained in mtDNA molecules that have the common ~13 kb deletion. Targeting the primers to non-deleted region enables amplification of all partly deleted molecules. Total DNA was isolated from snap-frozen QF by standard proteinase K and phenol-chloroform methods and was amplified from 10 ng of total DNA with the primers GAGGTGATGTTTTGGTAAACA GGCGGGGT and GGTTTCGTTTGTTC AACGATTAAAGT CCTACGTG by using Phusion DNA polymerase (Finnzymes) and buffer GC. Reaction conditions were the following: initial denaturation of 30 s at 98°C; 22 cycles of 10 s at 98°C and 3 min at 72°C and finally at 72°C for 10 min. For nuclear DNA control, we amplified GAPDH from 30 ng total DNA. With the use of nuclear control, it was possible to determine the relative amount of mtDNA in each sample by proportioning the mtDNA PCR product with the nuclear PCR product. GAPDH was amplified with primers TGGCCAAGGTCATC

CATGACA and CGTTCAGCTCTGGGATGACCT by DynaZyme DNA polymerase II (Finnzymes). The amplification conditions were: initial denaturation of 3 min at 94°C; 23 cycles of 30 s at 94°C, 30 s at 60°C and 1 min at 72°C; final extension step of 10 min at 72°C.

Large-scale mtDNA deletions are known to occur at a certain mtDNA region, between the origin of heavy-strand replication (O_H) and the ribosomal rRNA genes producing ~3 kb mtDNA molecules. Targeting the primers within the non-deleted section, it is possible to amplify both partly deleted and WT mtDNA molecules. Non-deleted mtDNA PCR was done to be able to compare the proportion of the deleted mtDNA with whole mtDNA pool. The primers ACC CCGCTGTTTACCAAAAACATCACCTC and ACGTACC ACTTTAATCGTTGAACAAACGAACC were designed to produce 549 kb sized product within the 3 kb non-deleted region. The non-deleted mtDNA region was amplified from 10 ng of genomic DNA using Phusion DNA polymerase (Finnzymes) and GC buffer. The PCR conditions were: initial denaturation of 30 s at 98°C; 21 cycles of 10 s at 98°C and 3 min at 72°C; final extension step of 10 min at 72°C.

PCR products were electrophoresed through 1% agarose gel and samples in the same gel were compared. The gels were scanned by Typhoon 9400 fluorescence scanner (Amersham Biosciences) and bands quantified by ImageQuant (Amersham Biosciences) software.

mtDNA quantification

Total DNA was isolated from snap-frozen QF by standard proteinase K and phenol–chloroform methods. MtDNA copy number level was analyzed by real-time quantitative PCR (Q-PCR). In mtDNA Q-PCR, 25 ng of total DNA was used as template and the amplification level of CytB gene (GCTTTCCACTTCATCTTACCATT and TGTTGGGTTG TTTGATCCTG) primers was normalized against the nuclear beta-actin gene (primers GGAAAAGAGCCTCAGGGCAT and GAAGAGCTATGAGCTGCCTGA). The PCR reaction was performed using F-415L DyNAmo™ Flash SYBR® Green QPCR Kit (Finnzymes), and run on an Abi Prism SDS 7000 machine (Applied Biosystem). Amplification conditions were: 95°C for 7 min, followed by 35 cycles of 95°C for 10 s and 60°C for 30 s.

Citrate synthase analysis

Skeletal muscle samples for citrate synthase activity were analyzed as in Trounce *et al.* (14).

Blood analysis

The blood glucose (Precision Xceed, MediSense) and whole-blood lactate levels (Accutrend lactate, Roche) were tested in blood drawn from the tail vein after 3 months of diet. Terminal blood samples were collected under anesthesia with cardiac puncture when mice were sacrificed. Mice were anesthetized with 1.5 mg/kg Ketalar® (Pfizer) and 1 mg/kg Domitor® (Orion Pharma). Blood in lithium-heparin tubes was kept on ice until centrifugation at 6000g for 10 min at

+4°C. Plasma was transferred to 1.5 ml tubes and kept frozen (−20°C) until analysis. Plasma was analyzed for glucose, sodium (Na), potassium (K), cholesterol, iron (Fe), triglycerides, inorganic phosphate (Pi), transaminases (aspartate aminotransferase, alanine aminotransferase and alkaline phosphatase), lactate dehydrogenase, glutamyl transferase, creatinine, chloride (Cl), amylase, creatinine kinase, calcium (Ca) and magnesium (Mg). Glucose, cholesterol, triglycerides and iron were only tested from fasted animals.

Blue native gel electrophoresis

Mitochondrial proteins were extracted from a piece of QF as described (15), and the concentrations were measured by the Bradford method. The samples were then stored in 750 mM aminocaproic acid and 5% Serva blue G (Serva) in aliquots at −80°C. Typically, 10 µg of protein of sample was loaded onto a gel. The samples were separated on a 6–15% blue native polyacrylamide gel electrophoresis (16,17), and blotted onto a PVDF membrane (Millipore) using standard semi-dry methods. For protein detection, we used monoclonal antibodies (Mitosciences) against the 39 kDa subunit of complex I and the 70 kDa subunit of complex II as a loading control. In-gel complex I activity was measured as described previously (18). Briefly, after blue native electrophoresis, the gel was incubated at room temperature first in 0.1 M Tris–HCl, pH 7.4, for 10 min, and then in 10 ml of reaction solution (0.2 mM NADH and 1 mg/ml Nitro Tetrazolium Blue (Sigma-Aldrich) in 0.1 M Tris–HCl, pH 7.4) until a purple precipitate formed, indicating enzymatic activity. Complex I activity was quantified by measuring the band intensity with a GS-800 Calibrated Densitometer (Bio-Rad) and Quantity One® 1-D analysis software (Bio-Rad).

Gene expression analyses

Total cellular RNA was extracted from frozen tissue samples in TRIzol reagent (Invitrogen) and homogenized with Dounce homogenizer with 30 consecutive strokes. One microgram of total RNA was used to generate cDNA using random hexamers with Moloney Murine Leukemia Virus Reverse Transcriptase (Promega). Quantitative real-time PCRs were performed on cDNA generated from mouse tissues with a DyNAmo Flash SYBR Green qPCR Kit (Finnzymes) on an ABI prism 7000 light cycler, and quantification was confirmed to be specific and exponential. Primer sequences used in this study were: UCP3 forward 5' CGAATTGGCCTCTACGA 3' and UCP3 reverse 5' TGTAGGCATCCATAGTCCC 3'; beta-actin forward 5' ATGCTCCCCGGGCTGTAT 3' and beta-actin reverse 5' CATAGGAGTCCTTCTGACCCATTC 3'.

Metabolomic analysis using the GCxGC-TOF/MS platform

To 15.3–19.8 mg samples, 20 µl of an internal standard-labeled palmitic acid (16:0–16,16,16d₃; 258 mg/l) and 400 µl of methanol solvent were added. Samples were ground and extracted with a Retsch Mixer Mill Type MM 301 for 5 min at 25 Hz. After incubating for 30 min at room temperature, the supernatant was separated by centrifugation

at 10 000 rpm for 5 min. The sample was dried under constant flow of nitrogen gas. To the dried sample, 25 μ l of MOX (2% methoxyamine HCl in pyridine) was added. The mixture was then incubated at 45°C for 1 h and derivatized with 25 μ l of MSTFA (*N*-methyl-*N*-(trimethylsilyl)trifluoroacetamide) by incubating at 45°C for 1 h. To the metabolite mixture, 5 μ l of retention index standard mixture with five alkanes at 150 ppm was added. Sample order for analysis was established by randomization. The instrument used was a GCxGC-TOF mass spectrometer (Pegasus 4D; Leco) with an autosampler (6890N GC and Combi PAL; Agilent Technologies). The instrument parameters were as follows: 1 μ l split injection 1:20; first column, RTX-5, 10 m \times 180 μ m \times 0.20 μ m; second column, BPX-50, 1.50 m \times 100 μ m \times 0.10 μ m; helium 39.6 psig constant pressure; temperature programs, primary oven, initial 50°C, 1 min \rightarrow 295°C, 7°C/min, 3 min, and secondary oven, 20°C above primary oven temperature; second-dimension separation time 5 s; MS measurement 45–700 amu, 100 spectra/s. Raw data were processed using ChromaTOF software (Leco), followed by alignment and normalization using the in-house-developed software. Unwanted background peaks were eliminated using the classification feature of ChromaTOF software. In-house-developed software was used to perform additional filtering using compound identifications by ChromaTOF. The metabolites were identified using an in-house reference compound library as well as by searching the reference mass spectral library. Mass spectra from the GCxGC-TOF/MS analysis were searched against The Palisade Complete Mass Spectral Library, 600K Edition (Palisade Mass Spectrometry). The matches to reference spectra are based on a weighted dot product of the two spectra, with higher *m/z* peaks having more weight than the lower. A similarity value is assigned between 0 and 999, with 999 being a perfect match and 750 generally considered as a reasonable match. We used the conservative cut-off criterion of 850 for identification.

Lipidomic analysis

Plasma samples (20 μ l) were extracted with chloroform/methanol (2:1, 100 μ l) after addition of an internal standard mixture containing 10 lipid compounds. The samples were centrifuged (10 000 rpm, 3 min), and 60 μ l of the lower lipid extract was taken into an HPLC vial insert and another standard mixture containing three labeled lipid compounds was added. The internal standards include PC(17:0/0:0), PC(17:0/17:0), PE(17:0/17:0), PG(17:0/17:0)[rac], Cer(d18:1/17:0), PS(17:0/17:0), PA(17:0/17:0) and *D*-erythro-sphingosine-1-phosphate (C17 Base) from Avanti Polar Lipids (Alabaster, AL, USA) and MG(17:0/0:0/0:0)[rac], DG(17:0/17:0/0:0)[rac] and TG(17:0/17:0/17:0) from Larodan Fine Chemicals (Malmö, Sweden). The labeled standards include PC(16:0/0:0-D3), PC(16:0/16:0-D6) and TG(16:0/16:0/16:0-¹³C) from Larodan Fine Chemicals (Malmö, Sweden).

Lipid extracts (2 μ l injections) were analyzed on a Waters Q-ToF Premier mass spectrometer combined with an Acquity Ultra Performance LCTM (UPLC) (Waters Inc., Milford, MA, USA). The column was an Acquity UPLCTM BEH C18 10 \times 50 mm with 1.7 μ m particles and the gradient solvent

system included water (1% 1 M NH₄Ac, 0.1% HCOOH) and LC/MS grade (Rathburn) acetonitrile/isopropanol (5:2, 1% 1 M NH₄Ac, 0.1% HCOOH). The total run time including a 5 min re-equilibration step was 18 min. The flow rate was 0.200 ml/min. The data were collected at a mass range of *m/z* 300–1200 with a scan duration of 0.2 s in the ESI+ mode. The peaks were processed using MZmine 0.60 software (19) and calibrated with internal standards as described previously (20).

SUPPLEMENTARY MATERIAL

Supplementary Material is available at *HMG* online.

ACKNOWLEDGEMENTS

The authors would like to thank Brendan Battersby for his advice, Anders Paetau and Hannu Kalimo for their expertise and help with muscle histopathology, Sinikka Tähkä for technical advices and Anu Harju and Ilse Lappalainen for technical help.

Conflict of Interest statement. None declared.

FUNDING

This work was supported by Sigrid Juselius Foundation, Jane and Aatos Erkko Foundation, Centre of Excellence Program of the Academy of Finland, Finnish Institute of Molecular Medicine, University of Helsinki (for A.S.) and Helsinki Biomedical Graduate School (for S.A.-E).

REFERENCES

- Chinnery, P., Majamaa, K., Turnbull, D. and Thorburn, D. (2006) Treatment for mitochondrial disorders. *Cochrane Database Syst. Rev.*, Art. No.: CD004426. doi:10.1002/14651858.CD004426.pub2.
- Tyynismaa, H., Mjosund, K.P., Wanrooij, S., Lappalainen, I., Ylikallio, E., Jalanko, A., Spelbrink, J.N., Paetau, A. and Suomalainen, A. (2005) Mutant mitochondrial helicase Twinkle causes multiple mtDNA deletions and a late-onset mitochondrial disease in mice. *Proc. Natl Acad. Sci. USA*, **102**, 17687–17692.
- Spelbrink, J.N., Li, F.Y., Tiranti, V., Nikali, K., Yuan, Q.P., Tariq, M., Wanrooij, S., Garrido, N., Comi, G., Morandi, L. *et al.* (2001) Human mitochondrial DNA deletions associated with mutations in the gene encoding Twinkle, a phage T7 gene 4-like protein localized in mitochondria. *Nat. Genet.*, **28**, 223–231.
- Suomalainen, A., Majander, A., Haltia, M., Somer, H., Lonnqvist, J., Savontaus, M.L. and Peltonen, L. (1992) Multiple deletions of mitochondrial DNA in several tissues of a patient with severe retarded depression and familial progressive external ophthalmoplegia. *J. Clin. Invest.*, **90**, 61–66.
- Santra, S., Gilkerson, R.W., Davidson, M. and Schon, E.A. (2004) Ketogenic treatment reduces deleted mitochondrial DNAs in cultured human cells. *Ann. Neurol.*, **56**, 662–669.
- Kang, H.C., Lee, Y.M., Kim, H.D., Lee, J.S. and Slama, A. (2007) Safe and effective use of the ketogenic diet in children with epilepsy and mitochondrial respiratory chain complex defects. *Epilepsia*, **48**, 82–88.
- Joshi, C.N., Greenberg, C.R., Mhanni, A.A. and Salman, M.S. (2009) Ketogenic diet in Alpers–Huttenlocher syndrome. *Pediatr. Neurol.*, **40**, 314–316.
- Bough, K.J., Wetherington, J., Hassel, B., Pare, J.F., Gawryluk, J.W., Greene, J.G., Shaw, R., Smith, Y., Geiger, J.D. and Dingledine, R.J. (2006) Mitochondrial biogenesis in the anticonvulsant mechanism of the ketogenic diet. *Ann. Neurol.*, **60**, 223–235.

9. Garcia-Roves, P., Huss, J.M., Han, D.H., Hancock, C.R., Iglesias-Gutierrez, E., Chen, M. and Holloszy, J.O. (2007) Raising plasma fatty acid concentration induces increased biogenesis of mitochondria in skeletal muscle. *Proc. Natl Acad. Sci. USA*, **104**, 10709–10713.
10. Surwit, R.S., Feinglos, M.N., Rodin, J., Sutherland, A., Petro, A.E., Opara, E.C., Kuhn, C.M. and Rebuffe-Scrive, M. (1995) Differential effects of fat and sucrose on the development of obesity and diabetes in C57BL/6J and A/J mice. *Metabolism*, **44**, 645–651.
11. Wenz, T., Diaz, F., Spiegelman, B.M. and Moraes, C.T. (2008) Activation of the PPAR/PGC-1alpha pathway prevents a bioenergetic deficit and effectively improves a mitochondrial myopathy phenotype. *Cell Metab.*, **8**, 249–256.
12. Kennedy, A.R., Pissios, P., Otu, H., Xue, B., Asakura, K., Furukawa, N., Marino, F.E., Liu, F.F., Kahn, B.B., Libermann, T.A. *et al.* (2007) A high-fat, ketogenic diet induces a unique metabolic state in mice. *Am. J. Physiol. Endocrinol. Metab.*, **292**, E1724–E1739.
13. Folch, J., Lees, M. and Sloane Stanley, G.H. (1957) A simple method for the isolation and purification of total lipides from animal tissues. *J. Biol. Chem.*, **226**, 497–509.
14. Trounce, I.A., Kim, Y.L., Jun, A.S. and Wallace, D.C. (1996) Assessment of mitochondrial oxidative phosphorylation in patient muscle biopsies, lymphoblasts, and transmittochondrial cell lines. *Methods Enzymol.*, **264**, 484–509.
15. Lyly, A., Marjavaara, S.K., Kyttala, A., Uusi-Rauva, K., Luiro, K., Kopra, O., Martinez, L.O., Tanhuanpaa, K., Kalkkinen, N., Suomalainen, A. *et al.* (2008) Deficiency of the INCL protein Ppt1 results in changes in ectopic F1-ATP synthase and altered cholesterol metabolism. *Hum. Mol. Genet.*, **17**, 1406–1417.
16. Schagger, H., Aquila, H. and Von Jagow, G. (1988) Coomassie blue-sodium dodecyl sulfate-polyacrylamide gel electrophoresis for direct visualization of polypeptides during electrophoresis. *Anal. Biochem.*, **173**, 201–205.
17. Wittig, I., Braun, H.P. and Schagger, H. (2006) Blue native PAGE. *Nat. Protoc.*, **1**, 418–428.
18. Zerbetto, E., Vergani, L. and Dabbeni-Sala, F. (1997) Quantification of muscle mitochondrial oxidative phosphorylation enzymes via histochemical staining of blue native polyacrylamide gels. *Electrophoresis*, **18**, 2059–2064.
19. Katajamaa, M., Miettinen, J. and Oresic, M. (2006) MZmine: toolbox for processing and visualization of mass spectrometry based molecular profile data. *Bioinformatics*, **22**, 634–636.
20. Laaksonen, R., Katajamaa, M., Paiva, H., Sysi-Aho, M., Saarinen, L., Junni, P., Lutjohann, D., Smet, J., Van Coster, R., Seppanen-Laakso, T. *et al.* (2006) A systems biology strategy reveals biological pathways and plasma biomarker candidates for potentially toxic statin-induced changes in muscle. *PLoS ONE*, **1**, e97.